Predictability of hydrogen-based mixtures detonations in thin channels: new experiments and improvements in the quasi-two-dimensional model

Farzane Zangene, Aliou Sow, Matei Radulescu
University of Ottawa
Ottawa, Ontario, Canada

1 Introduction

The propagation of detonations in tubes/channels is subjected to wall losses in the form of mass divergence to the boundary layers that causes velocity deficit [1]. Progress in knowing the detonation structure has relied upon conducting experiments in narrow channels, however, it is desirable to have a computational method to simulate detonation propagation and draw conclusions between experimental and computational results. The three-dimensional simulation of gaseous detonation [2] for modelling viscous boundary layer requires a highly refined grid resolution due to the thin boundary layer which uses excessive resources and is computationally expensive. Although the one-dimensional [3] simulation of the detonation losses are less expensive, detonation waves in narrow channels are usually observed to have a quasi-two-dimensional structure. Characterization of the boundary layer is important to accurately predict the detonation dynamics in such narrow channels.

Recently, Xiao et *al.* [4] proposed a novel quasi-2D model to reconstruct the two-dimensional cellular structures of detonation waves. Their proposed model incorporates an area divergence term in the reactive Euler equations to account for the boundary layer losses. The area divergence term is evaluated from Fay's boundary layer theory [5] by using Mirels' laminar boundary layer solution [6]. To obtain a good agreement between the experiment and the simulation, Mirels' constant was decreased by a factor of 2.3 in their model. In Mirels' model, the flow behind the shock is considered steady, with a constant mean stream velocity. However, behind the lead shock of detonation waves, the flow is non-uniform. We attempt here to improve upon Xiao's model [4] by taking into consideration the role of the unsteady effects. With the new version of the quasi-2D model proposed here, the Mirels's constant needs only to be modified by a factor of 1.3 to reproduce the recorded experimental cell size.

2 Experiment

Experiments were conducted in a 3.4-m-long thin aluminum channel with an internal cross-section height and width of 0.203 m and 0.019 m, respectively. The rectangular shock tube comprises three parts, i.e., the detonation initiation section, the propagation section, and the glass-equipped test section for visualization purposes, as detailed elsewhere [7]. The premixed combustible mixture was ignited

Correspondence to: fzang055@uottawa.ca

in the first part by a capacitor discharge. Inserted mesh wires ensured a detonation was formed in the first section of the tube. Subsequently, detonations travelled in the second propagation part and then entered the third test section. The propagation process was then visualized by utilizing the classical Z-type schlieren technique with the Phantom v1210 camera at 77108 frames per second (about 12.9 μs for each interval). The schlieren visualization was implemented with a vertical knife-edge utilizing a light source of 360 W, with the exposure time set to 0.44 μs and the frame resolution kept at 384 $\times$ 288 px. Eight high-frequency piezoelectric PCB pressure sensors were installed on the shock tube's top wall to record pressure signals. The average of the repeated experiments' global velocity was considered as the detonation velocity and used in calculations. Pilot tests had been done to avoid an overdriven detonation wave in the test section due to the high-pressure driver gas and the lowest pressure that initiated detonation waves was determined. The ratio of 2.37 between driver gas and test gas was kept constant in all the experiments as the reference for filling the shock tube [8]. Two different hydrogen-oxygen mixtures were tested, stoichiometric hydrogen-oxygen-argon ($2H_2/O_2/7Ar$), and stoichiometric hydrogen-oxygen-helium ($2H_2/O_2/7He$). Each mixture was prepared in a separate mixing tank by the method of partial pressures and was then left to mix for more than 24 hours. The shock tube was evacuated to a pressure below 80Pa before filling it with driver and test gases. The initial pressure of the test gases was adjusted in which the induction zone length calculated from the ideal ZND model is constant between the two different mixtures. Considering the classical correlation between cell size and induction zone length, ideally, we expected to observe the same cellular structure between two mixtures. In table 1, the experimental conditions with the one-dimensional ZND induction zone length, the global average velocity deficit measured from pressure sensors and the average cell size measured from videos are presented.

Table 1: Experimental mixtures and conditions.

Test Mixture	P_0 [kPa]	T_0 [K]	Δ_i [mm]	D/D_{CJ}	Cell Width [mm]
$2H_2 + O_2 + 7AR$	4.1	295	2.83	0.8	203
$2H_2 + O_2 + 7HE$	9.3	295	2.83	0.86	94

Figure 1 shows the superimposed schlieren photos of a sequence of frames in two different bath gases for different initial pressures. The experimental measurements of the cell width show that the difference between the argon and helium is approximately 53%. These results reveal that close to the limit, lengthening in the reaction zone reduces the velocity of the wave, which causes the discrepancy in the size of the cells between two mixtures [8].

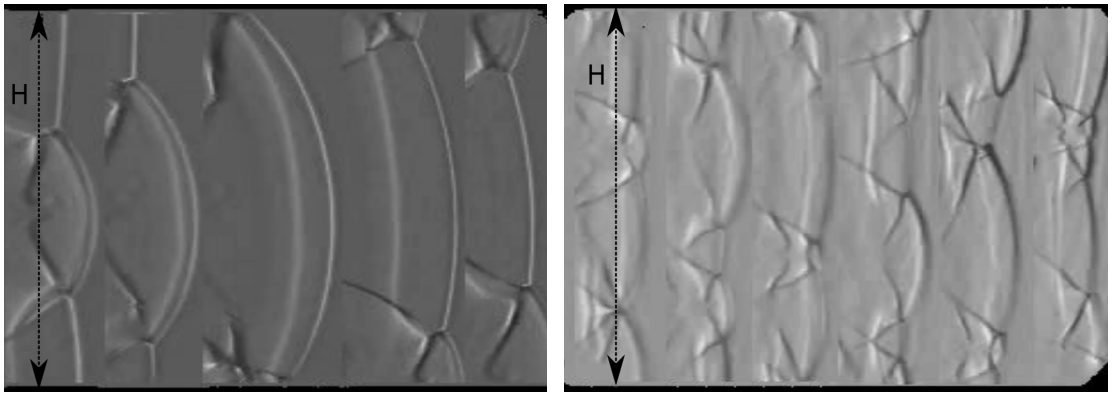

Figure 1: Superposition of detonation fronts at different instants along the shock tube. Left: argon dilution, P_0= 4.1 kPa . Right: helium dilution, P_0= 9.3 kPa, H is the channel height of 203 mm.

3 Modelling

In this study, the reactive two-dimensional Euler equations supplemented by a source term to model the boundary layer effects are used as governing equations [4]. The viscous boundary layer developing behind a detonation wave leads to an apparent cross-sectional increase as illustrated in Fig. 2. The source term is proportional to $\frac{D(\ln A)}{Dt}$.

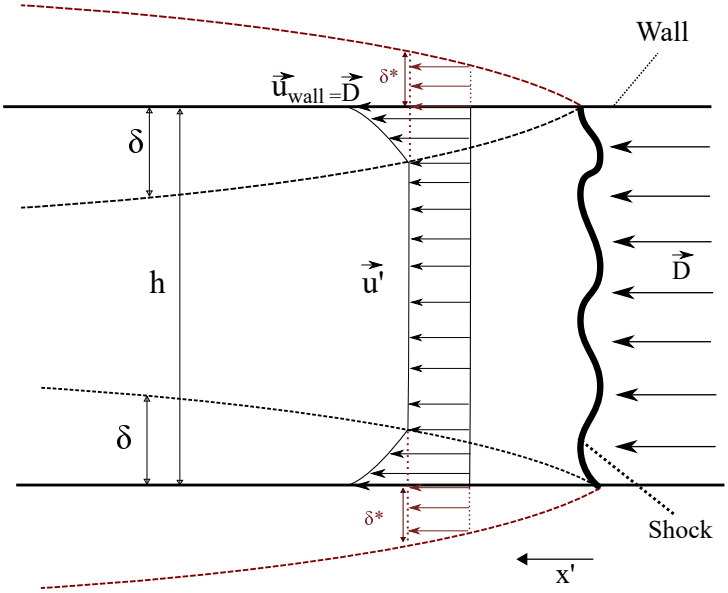

Figure 2: The steady flow in post-shock region of a detonation wave in the shock attached reference frame. The dashed lines inside the walls indicate the outer edges of the boundary layer (δ) and the dashed lines outside of the walls indicate the outer edges of the displaced boundary layer ($\delta^\star$). h is the channel height in the z-direction, D is the detonation speed, x' is the distance in the post-shock region in the shock attached frame and u' is the post-shock region velocity.

In the shock attached reference frame, the source term will be proportional to:

$$\frac{D(\ln A)}{Dt} = \frac{\partial(\ln A)}{\partial t'} + u' \frac{\partial(\ln A)}{\partial x'} = \frac{1}{A}\frac{\partial A}{\partial t'} + u' \frac{1}{A}\frac{\partial A}{\partial x'} \tag{1}$$

The motion is assumed to be pseudo-steady, hence, the term $\frac{\partial A}{\partial t'}$ in Eq. 1 is neglected to the leading order. According to the Mirels' theory, the laminar boundary layer displacement thickness and its derivative with respect to x' (distance from the post shock region) is as follow:

$$\delta^\star(x') = K_M \sqrt{\frac{\mu_s}{\rho_s u'}} x'^{\frac{1}{2}} \qquad ; \qquad \frac{d\delta^\star(x')}{dx'} = \frac{K_M}{2} \sqrt{\frac{\mu_s}{\rho_s u'}} x'^{\frac{-1}{2}} \tag{2}$$

in which u', ρ_s and μ_s are the velocity in the shock attached reference frame, the density and, the viscosity in the post-shock region, respectively. K_M is the Mirels constant.

Replacing $A = h + 2\delta^\star(x')$ in Eq. 1:

$$\frac{1}{A}\frac{\partial A}{\partial x'} = \frac{1}{h + 2\delta^\star(x')} 2 \frac{d\delta^\star(x')}{dx'} \tag{3}$$

Using Eq. 2 in Eq. 3 one obtains:

$$\frac{D(\ln A)}{Dt} = \frac{k_M}{h}\sqrt{\frac{\nu_s}{t'}} \tag{4}$$

In Eq. 4, t' represents the time elapsed since the particle passed through the shock. To determine the elapsed time, Xiao et al. [4] used a non-advected passive scalar. As in Mirels' model, the state behind the shock is assumed to be constant. In the present work, we propose to generalize Xiao et al. [4] model by considering the changes in the upstream velocity. To this end, we use an advected passive scalar to account for flow non-uniformities behind the shock. The time at which the particle crosses the shock, t_s, is defined as follow:

$$\frac{Dt_s}{Dt} = 0 \tag{5}$$

By identifying that $t' = t - t_s$, one obtains from Eq. 5 after few algebraic manipulations:

$$\frac{\partial t'}{\partial t} = 1 - U\frac{\partial t'}{\partial x} \tag{6}$$

U is the velocity of the flow measured in laboratory reference frame in the post-shock region and t' is the elapsed time since a particle has passed through the shock front as illustrated in Fig. 3.

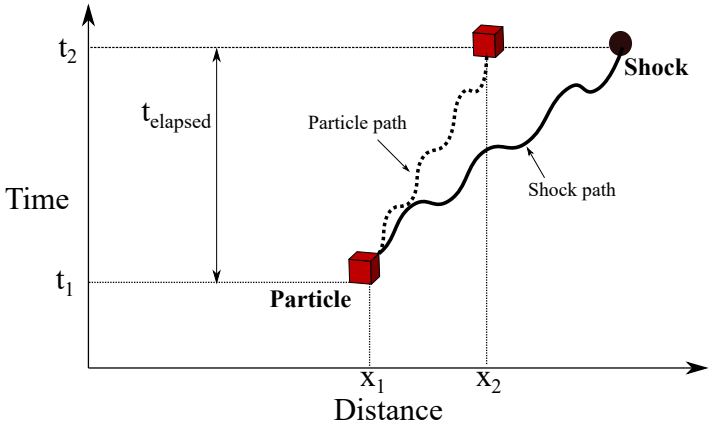

Figure 3: Advection of a particle in post shock region with time and distance.

3 Numerical simulation

A second-order-accurate exact Godunov solver [9] with adaptive mesh refinement [4] is used to solve the governing equations. To model the chemical kinetics, the two-step chain-branching reaction model (the thermally neutral induction zone followed by the exothermic reaction zone) was employed and the non-dimensional parameters for the two-step model were calibrated from the detailed chemistry by using the San Diego chemical reaction mechanism provided in Shepherd's Shock and Detonation Toolbox (SDToolbox) [10]. The induction zone length is kept constant for both helium and argon experiments. The channel height is nondimensionalized by the induction zone length. To make sure that we cover the length of the shock tube, 3.4 m, a domain length of $2500\Delta_i$ is considered for the simulations. For reference, the induction zone length is 0.0028 meters. In these simulations, the detonation propagates from left to the right, with reflective boundary conditions imposed on the top and bottom sides, and zero-gradient boundary conditions applied to the left and right ends.

Table 2 shows the non-dimensional parameters for the two-step chemistry model for the two different mixtures. In this table γ is the isentropic exponent in the post-shock state, E_a is the activation energy, Q is the heat release, and k_i and k_r are rate constant controlling the induction and reaction zones, respectively.

Table 2: The calibrated non-dimensional parameters for the two-step model from the detailed chemistry.

Test Mixture	P_0	γ	E_a/RT_0	Q/RT_0	k_i	k_r
$2H_2 + O_2 + 7AR$	4.1	1.5	31.16	11.5	45.5	0.07
$2H_2 + O_2 + 7HE$	9.3	1.5	23.98	11.9	12.38	0.13

3.1 Result

Below is the result of the 2D simulations for both diluents argon and helium, in which the simulation reproduces the same cellular structure as the experiments. The velocity deficits are measured on the top wall in nine repeating cycles. The average velocity deficit D/D_{CJ}= 0.85 for $2H_2/O_2/7$Ar and D/D_{CJ}= 0.91 for $2H_2/O_2/7$He are measured. The open shutter photograph from the simulation which records the maximum energy release rates is shown in Fig. 4. The measured cell sizes from the nine repeating cycles are λ= 203 mm and λ= 82 mm for the argon and helium dilution, respectively.

The theoretical Mirels' constant for the mixture $2H_2/O_2/7$Ar at P_0= 4.1 kPa is K_M= 4, however, the present simulations show that K_M= 3 can very well recover the cellular structure of the experiments. To have the same effects of the modelling of losses in the mixture $2H_2/O_2/7$He, the ratio between theoretical and measured K_M from argon mixture, $K_{M_{theoretical}}/K_{Msimulation}$= 1.3, is kept constant for the $2H_2/O_2/7$He mixture which gives K_M= 2.8.

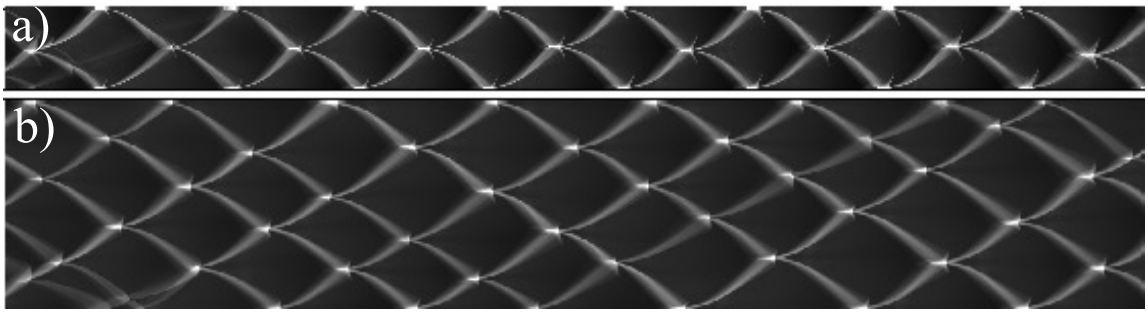

Figure 4: The recorded maximum energy release rates of detonations in a) $2H_2/O_2/7$Ar at P_0= 4.1 kPa with cell size λ= 203 mm, and K_M= 3, b) $2H_2/O_2/7$He with cell size λ= 82 mm, K_M= 2.8. The length of the shown domain is 1100 Δ_i for a) and 400Δ_i for b).

In Xiao *et al.* 2D simulations [4] in $2H_2/O_2/7Ar$ at P_0= 4.1 kPa to reproduce the experiment cellular structure, the theoretical Mirels' constant K_M was decreased by 56%. However, with the proposed improvement model K_M is only decreased by 25%.
To visualize qualitative features of the detonation structure, the temporal velocity evolution at a single cell is reconstructed from simulation as shown in Fig. 5. In addition to the reproduction of the velocity deficit and cell size, the cellular dynamics are very well reproduced compared to the experiments (bottom row).

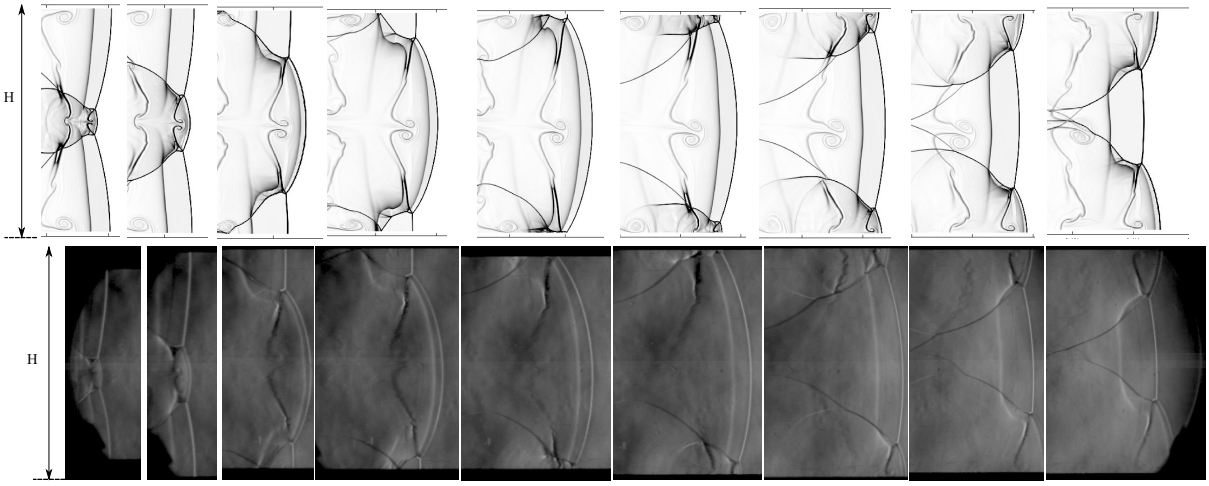

Figure 5: Comparisons of the gradient of the density for argon dilution at P_0= 4.1 kPa between the quasi-2D simulation (top) with the schlieren photos of the experiment (bottom). H is the channel height of 203 mm.

In Fig. 6 the velocity deficits measured from the ZND model with losses (lines), experiments (circles) and 2D simulation (squares) for both mixtures versus nondimensionalized induction zone length (nondimensionalized with channel width) are presented. The error bars are experimental errors calculated between repeated experiments in the same mixture and the same initial pressure five times. For argon dilution, an error of 0.63% is calculated while for the helium mixture an error of 1.2% is obtained. Although the quasi-2D simulation predicts the cell size measured by the experiment very well, it under-predicts the velocity deficit.

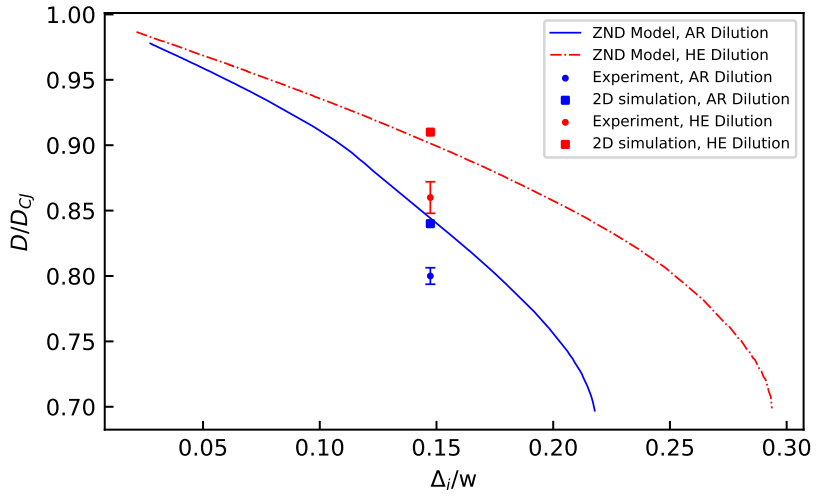

Figure 6: Comparisons of the measured velocity deficit in quasi-2D simulation, the steady 1D ZND model with loss and experiments versus nondimensionalized induction zone length.

4 Conclusion

In narrow channels, the boundary layers have an important role in the detonation dynamics. The high numerical resolution required to accurately capture the viscous boundary layer often constitutes a challenge to direct numerical simulations. Quasi-2D simulations can help to overcome this challenge. In this study, we have proposed a modified version of the quasi-2D model proposed previously in another work [4]. The proposed modification takes into account the fact that the flow velocity is not uniform downstream of the detonation waves. Finally, the comparison of the results of the modified quasi-2D model with experimental results indicates that the cell size can be predicted by modifying the theoretical Mirels constant by only a factor of 1.3.

References

[1] J. Lee, *The Detonation Phenomenon*. Cambridge University Press, 2008.

[2] C. Wang, C.-W. Shu, W. Han, and J. Ning, "High resolution weno simulation of 3D detonation waves," *Combustion and Flame*, vol. 160, pp. 447–462, 2013.

[3] Y. Zeldovich, *On the theory of the propagation of detonation in gaseous systems*. NACA Technical Report, 1950.

[4] Q. Xiao, A. Sow, B. M. Maxwell, and M. I. Radulescu, "Effect of boundary layer losses on 2D detonation cellular structures," *Proceedings of the Combustion Institute*, vol. 38, pp. 3641–3649, 2021.

[5] J. Fay, "Two Dimensional Gaseous Detonations:Velocity Deficit," *Physics of Fluids*, vol. 2(3), p. 283, 1959.

[6] H. Mirels, *Boundary layer behind shock or thin expansion wave moving into stationary Fluid*. NACA TN 3712, 1956.

[7] Q. Xiao and M. I. Radulescu, "Dynamics of hydrogen–oxygen–argon cellular detonations with a constant mean lateral strain rate," *Combustion and Flame*, vol. 215, pp. 437–457, 2020.

[8] X. Q. Zangene F, Hong Z and R. M, "The role of the argon and helium bath gases on the detonation structure of hydrogen oxygen mixtures," *International Conference on Hydrogen Safety, Edinburgh*, 2021.

[9] S. Falle, "Self similar jets," *Monthly Notices of the Royal Astronomical Society*, vol. 250(3), 1991.

[10] "Chemical mechanism: Combustion research group at uc san diego," 2014.